Enhancement of fracture toughness in nanostructured diamond–SiC composites

Yusheng Zhao,[a] Jiang Qian, Luke L. Daemen, Cristian Pantea, and Jianzhong Zhang
LANSCE Division, Los Alamos National Laboratory, Los Alamos, New Mexico 87544

Georgiy A. Voronin and T. Waldek Zerda
Department of Physics & Astronomy, Texas Christian University, Fort Worth, Texas 76129

(Received 17 October 2003; accepted 31 December 2003)

We synthesized diamond–SiC nanocomposites with superhardness *and* greatly enhanced fracture toughness through a synthetic approach based on high-energy ball milling to form amorphous Si precursors followed by rapid reactive sintering at high pressure (P) and high temperature (T). We show how the simultaneous $P-T$ application allows for better control of the reactive sintering of a nanocrystalline SiC matrix in which diamond crystals are embedded. The measured fracture toughness K_{IC} of the synthesized composites has been enhanced greatly, as much as 50% from 8.2 to 12.0 MPa $m^{1/2}$, as the crystal size of the SiC matrix decreases from 10 μm to 20 nm. Our result contradicts a commonly held belief of an inverse correlation between hardness and fracture toughness. We demonstrate the importance of nanostructure for the enhancement of mechanical properties of the composite materials. © *2004 American Institute of Physics.*
[DOI: 10.1063/1.1650556]

With a Vicker's hardness up to 100 GPa, diamond is the hardest material known to mankind.[1,2] Diamond also has the highest bulk modulus (443 GPa) and the highest shear modulus (535 GPa) among all materials.[1] However, diamonds are brittle with a low fracture toughness of 3–5 MPa $m^{1/2}$ for single crystals. This flaw limits the use of diamonds for applications in harsh environments of dynamic impacts and high stress concentrations.

The sintering of polycrystalline diamond composites under high $P-T$ conditions can enhance fracture toughness without much compromising hardness and wear resistance.[3] The fracture toughness of polycrystalline diamond composites ranges from 6 to 9 MPa $m^{1/2}$ depending on sintering conditions and the bonding matrix.[3–6] The diamond–SiC composite is of great interest for its higher thermal stability compared to traditional Co- and Ni-bonded diamond composites.[7–9] The design of nanostructured diamond–SiC composites with enhanced fracture toughness, while maintaining superhard and superabrasive properties, is the focus of present study.

We have investigated three sample preparation procedures for the high $P-T$ synthesis of diamond–SiC composites: (1) high-energy ball milling of a mixture of diamond and silicon; (2) thorough wet mixing in methanol; and (3) liquid/melt phase infiltration. The diamond+silicon initial mixture had a molar ratio of about 90:10. The SiC bonding matrix is formed via a chemical reaction between silicon and carbon (i.e., diamond) during the high $P-T$ reactive sintering. The diamond and silicon mixtures were sintered reactively at high $P-T$ conditions of 5 GPa and 1800 K for 30 s. The run products are well-sintered cylindrical chunks with a diameter of 5 mm and thickness of 3 mm. The median grain sizes were determined for the SiC matrix (Fig. 1) by the Scherrer's equation using all SiC Bragg peaks.[10,11]

In procedure 1, synthetic diamond powders of grain size 5–10 μm (General Electric Co.) and crystalline silicon powder of grain size 10–20 μm (Alfa Aesar) were used as starting materials for the mixture. The diamond+Si mixture was ball-milled under argon atmosphere for 11 h with a Certiprep Spex 8000-D mixer mill with tungsten carbide (WC) balls and vials. Experiments show that the participation of micron-size diamond particles in the ball-milling process greatly speeds up particle size-reduction and amorphous transformation of crystalline silicon. The Raman spectroscopy and x-ray diffraction data reveal that the crystalline silicon becomes completely amorphous after the ball-milling process. Simultaneously the diamond grains are uniformly coated with amorphous silicon. This mixture preparation procedure solves the ''bottle-neck'' problem existing in the traditional liquid/melt phase infiltration technique[12,13] (see procedure 3 of this study), in that the formation of SiC quickly blocks the ability of the Si melt to penetrate deeply into the nanoscale matrix. It also provides a large quantity of seed crystals to form the nanocrystalline SiC matrix from the initial amorphous state of Si, thus facilitating the SiC formation at high $P-T$ conditions and decreasing the amount of residual silicon in the sintered product.

Indentation experiments were carried out to measure the hardness ($H_v = 1.82\times10^7 \cdot F/D^2$ Pa, Ref. 14, converted to SI units) and fracture toughness ($K_{IC} = 0.1186 \cdot E^{1/2} \cdot F^{1/2} \cdot D/C^{3/2}$ Pa $m^{1/2}$, Ref. 15, converted to SI units) of the synthesis products using a Buehler Micro4 micron hardness tester, where F is the loading force in newtons, D the indentation diagonals in meters, E the elastic modulus in GPa, and C the crack length in meters.[14,15] For the high $P-T$ sintered sample prepared via procedure 1, there is no visible macrocrack formation under a microscope magnification of 1500× for loading forces up to 49 N. We observed that the measured

[a]Author to whom correspondence should be addressed; electronic mail: yzhao@lanl.gov

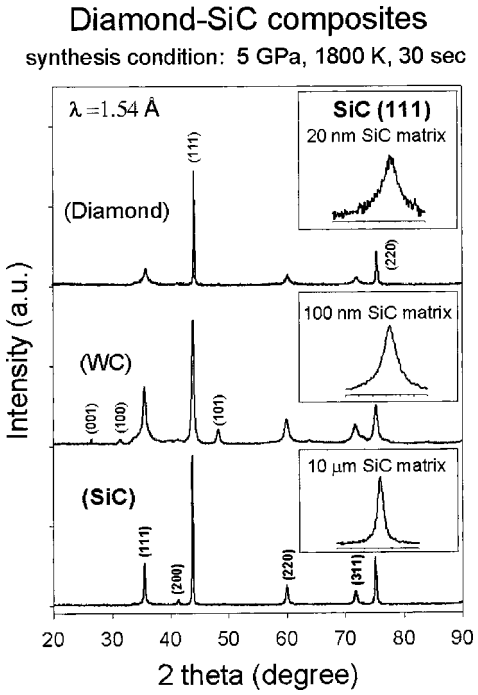

FIG. 1. X-ray diffraction patterns of diamond–SiC composites synthesized by means of three different procedures, ball milling (top), wet mixing (middle), and melt infiltration (bottom). The insets show the SiC (111) Bragg peak and illustrate the peak broadening induced by grain-size reduction. The weak WC peaks in the middle pattern are due to contamination of the starting mixture by WC balls and vials during wet mixing. No WC peaks were observed with procedure 1 because only the mixture of precursor materials from a second batch of ball milling was used for the high $P-T$ synthesis experiments, whereas the mixture from the first ball milling was discarded. This two-stage procedure allows WC balls and vials to be coated with precursor materials after the first milling, which effectively minimizes contamination in the subsequent ball milling process.

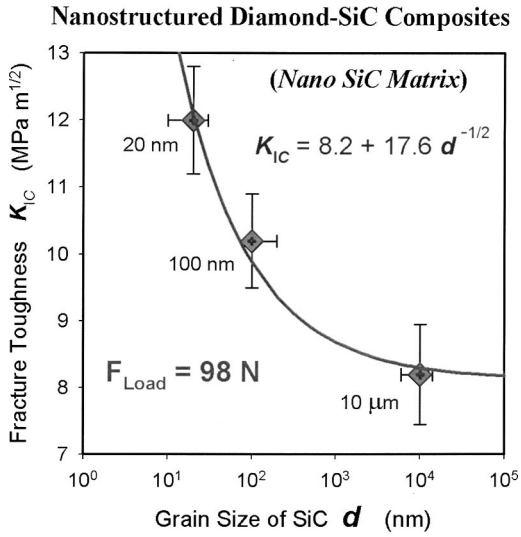

FIG. 2. Relationship between the fracture toughness of the diamond–SiC composite and the grain size of its SiC matrix. The diamonds indicate the measured fracture toughness values for the corresponding SiC grain sizes. All measurements are conducted at a constant loading force of $F_{\text{load}} = 98$ N. The curve, expressed by the equation $\mathbf{K}_{IC} = 8.2 + 17.6 \cdot d^{-1/2}$, represents a fit to the Hall–Petch relation. For self-consistency, previously reported fracture toughness values of diamond composites, which ranges from 6 to 9 MPa m$^{1/2}$ for micron matrix, are not plotted because they were measured at different loading forces and did not have consistency to reach the ''asymptotic hardness.'' For the same reason, we did not plot the only other experimental data on nanostructured diamond–SiC composites (Ref. 13), of which $\mathbf{K}_{IC} = 10 \pm 3$ MPa m$^{1/2}$ for an average grain size=20 nm of the SiC matrix.

hardness decreases as the loading force increases. The $H_v - F_{\text{load}}$ curve eventually bends over and levels off at higher loads—a behavior previously observed for hard and brittle materials.[16,17] The noticeable appearance of visible macro-cracks at the corners of the inverted pyramid impression occurs only at $F_{\text{load}} \geqslant 98$ N (*well past the bend in the loading curve*) during the indentation tests. For the sake of consistency, all hardness and fracture toughness measurements are carried out at this particular loading force on all the samples in the present study.

The measured hardness of the synthesized diamond–SiC composites in the present study falls in the range $H_v = 60-80$ GPa for the samples synthesized from procedures 1 and 3. However, the measured fracture toughness of the synthesized composites increases greatly, as much as 50%, as the crystal size of the SiC matrix decreases from 10 μm to 20 nm (Fig. 2). The achieved fracture toughness of $\mathbf{K}_{IC} = 12$ MPa m$^{1/2}$ for the diamond–SiC composites is significant; it is about 30% tougher than tungsten carbide,[18] which has the fracture toughness of 8.9 MPa m$^{1/2}$ and is a hard and tough material often used for harsh applications where brittle polycrystalline diamond compacts would not work. Our data on fracture toughness versus grain size of the SiC matrix show a good fit to the Hall–Petch law[19,20] (Fig. 2). This result shows experimental evidence showing the nanoscale effect on the fracture toughness for bulk composite material. An inverse relationship between hardness and fracture toughness is the general rule for most materials. The present experimental study provides a practical way to overcome this limitation and achieves super-hardness and high fracture toughness simultaneously.

During the high $P-T$ sintering, the micron-size diamond grains have gone through an ''annealing'' process, which hardens and strengthens the diamond crystals.[21] We hypothesize that the highly concentrated dislocations and vacancies in the surface layers of the micron-sized diamonds are almost completely consumed by the carbon–silicon reactions, leaving few weakening defects within the diamond crystals. This mechanism is probably one of the reasons for polycrystalline diamond composites having higher fracture strength than the single-crystal diamonds. The nano-matrix results in a situation where the size of a micro-crack is bigger than the size of the matrix nanocrystals. To grow further, a crack would have to grow around the crystals, which would decrease its ability to propagate. This mobility reduction thus leads to an increase in the fracture toughness of the diamond-SiC nanocomposites.

Fracture mechanics studies have suggested that the morphology and distribution of polycrystalline grains, instead of the grain size, are the key factors for crack deflection process.[22] We do observed clear differences among the morphology and distribution of diamond and SiC phases in the samples made from three different procedures. At this stage, however, we make no effort to differentiate the contribution from grain size, morphology, and distribution. It is because all of those factors are intrinsically correlated for the sintered composite materials. Much more work is needed to elucidate the mechanism of fracture toughness enhancement in

diamond–SiC composites, as illustrated in Fig. 2.

Our second synthetic procedure also produced the diamond–SiC nanocomposites with the nano-diamond grains and nano-SiC matrix.[23] The samples show a substantial increase in fracture toughness to 10.2 $\mathrm{MPa\,m^{1/2}}$. However, there is a significant reduction in hardness, by as much as 35%–50%, compared with the products of the first and third synthetic procedures. This could well be the result of the low mechanical quality of the nano-diamond starting materials, which may possess significant amounts of defects in the crystal grains. Also, it may be due to the fact that procedure 2 has relatively higher SiC concentration (28 wt %, compared to the 20 wt % in the other two procedures).

The third synthesis procedure relied on the use of micron-size powders. Indeed, upon using nano-diamonds with the liquid/melt phase infiltration, it fails totally because silicon melts cannot sufficiently infiltrate the highly compacted nano-diamonds. Furthermore, the formation of SiC closes the pores in the diamond compact to prevent further infiltration, a ''self-stop'' phenomenon,[13] and the remaining bare diamond surfaces are quickly graphitized at high temperatures. This is to be contrasted with our procedure 1 in which the ball-milled mixture of micron-size diamonds and silicon powders can disperse very fine, amorphous silicon powder uniformly around the diamond particles. The high $P-T$ reactive sintering then results in a nanostructured diamond–SiC composite of high uniformity, low porosity, minimum residual silicon, and minimal quantities of graphite.

The thermally induced crystallization of amorphous solids has been extensively applied in recent efforts to synthesize nanocrystalline films on ribbon substrates.[24] More recently, pressure has vigorously been promoted as an effective thermodynamic parameter that controls the crystallization process.[25] The formation of crystalline SiC nuclei from reaction between amorphous/molten Si and carbon is thermodynamically favored under high pressure, as the amorphous Si and/or its molten phase has a lower density and a higher compressibility than the crystalline SiC phase. However, the grain growth of a large number of crystalline SiC nuclei accompanied by long-range atomic rearrangements is kinetically hindered at high pressures. This balancing act between thermodynamics and kinetics leads to the formation of a nanocrystalline SiC matrix. The subtle interplay between pressure, temperature, and sintering time allows finer controls in formation of nanostructured diamond–SiC composites with nanocrystalline SiC matrix. Our approach overcomes grain-growth problems for bulk materials fabricated by conventional methods, where slow thermal annealing accompanied with rapid crystallization to micron-size consumes both nanocyrstallites and the amorphous matrix. This synthetic technique presents opportunities to design and develop superhard composite materials with a strong nanocrystalline bonding matrix and, conceivably, with improved fracture toughness, yield strength, and thermal stability.

Our extensive hardness and fracture toughness observations illustrated a peculiar but common behavior of hardness with loading force in hard and brittle materials. It is important to emphasize that the asymptotic leveling-off of the measured hardness value is commonly associated with population growth of micro-cracks in brittle materials upon the increase of loading force. Our reported hardness is the asymptotic value determined at the ultimate appearance and propagation of macro-cracks, where the fracture toughness of the materials is also measured. We strongly recommend that the hardness for brittle materials be reported after the visible propagation of macro-cracks, i.e., past the bend in the H_v-F_{load} curve, when hardness approaches its asymptotic value. This loading curve behavior is probably responsible for a wide disparity in the measured hardness and fracture toughness values reported in the literature. There is clearly a need for theoretical modeling to better grasp the physical nature and correlations of hardness and fracture toughness in this class of materials.

This work was performed under the auspices of the U.S. Department of Energy (DOE) under Contract No. W-7405-ENG-36 with the University of California. The LANL research projects of ''Novel Superhard Materials and Nanostructured Diamond Composites'' are supported by DOE-OIT_IMF and by DoD/DOE_MOU programs.

[1] R. Riedel, *Handbook of Ceramic Hard Materials* (Wiley-VCH, Weinheim, 2000).
[2] C. A. Brookes, in *The Properties of Diamond*, edited by J. E. Fields (Academic, London, 1979), Chap. 9, pp. 383–402.
[3] D. Miess and G. Rai, Mater. Sci. Eng., A **209**, 270 (1996).
[4] M. D. Drory, C. F. Gardinier, and J. S. Speck, J. Am. Chem. Soc. **74**, 3148 (1991).
[5] V. V. Brazhkin, A. G. Lyapin, S. V. Popova, Y. A. Klyuev, and A. M. Naletov, J. Appl. Phys. **84**, 219 (1998).
[6] E. A. Ekimov, S. Gierlotka, E. L. Gromnitskaya, J. A. Kozubowski, B. Palosz, W. Lojkowski, and A. M. Naletov, Inorg. Mater. (Transl. of Neorg. Mater.) **38**, 1117 (2002).
[7] A. E. Ringwood, Australia Patent 601561 (1988).
[8] Y. S. Ko, T. Tsurumi, O. Fukunaga, and T. Yano, J. Mater. Sci. **36**, 469 (2001).
[9] J. Qian, G. Voronin, T. W. Zerda, D. He, and Y. Zhao, J. Mater. Res. **17**, 2153 (2002).
[10] P. Scherrer, Gött. Nachr. **2**, 98 (1918).
[11] H. P. Klug and L. E. Alexander, *X-Ray Diffraction Procedures for Polycrystalline and Amorphous Materials* (Wiley-Interscience, New York, 1974).
[12] I. E. Clark and P. A. Bex, Indust. Diamond Rev. **1**, 43 (1999).
[13] E. A. Ekimov, A. G. Gavriliuk, B. Palosz, S. Gierlotka, P. Dluzewski, E. Tatianin, Y. Kluev, A. M. Naletov, and A. Presz, Appl. Phys. Lett. **77**, 954 (2000).
[14] D. Sherman and D. Brandon, *Handbook of Ceramic Hard Materials*, edited by R. Riedel (Wiley-VCH, Weinheim, 2000), Chap. 3., p. 86.
[15] G. R. Anstis, P. Chantikul, B. R. Lawn, and D. B. Marshall, J. Am. Cheram. Soc. **64**, 533 (1981).
[16] Y. Zhao, D. W. He, L. L. Daemen, J. Huang, T. D. Shen, R. B. Schwarz, Y. Zhu, D. L. Bish, J. Zhang, G. Shen, J. Qian, and T. W. Zerda, J. Mater. Res. **17**, 3139 (2002).
[17] D. B. Sirdeshmukh, L. Sirdeshmukh, K. G. Subhadra, K. Kishan Rao, and S. Bal Laxman, Bull. Mater. Sci. **24**, 469 (2001).
[18] J. L. Chermant, A. Deschanvres, F. Osterstock, Fract. Mech. Ceram. **4**, 891 (1978).
[19] E. O. Hall, Proc. Phys. Soc. London, Sect. B **64**, 747 (1951).
[20] N. J. Petch, J. Iron Steel Inst., London **173**, 25 (1953).
[21] C. S. Yan, H. K. Mao, W. Li, J. Qian, Y. Zhao, and R. Hemley, Science, in review (2003).
[22] K. T. Faber and A. G. Evans, Acta Metall. **31**, 565 (1983).
[23] G. A. Voronin, T. W. Zerda, J. Qian, Y. Zhao, D. He, and S. N. Dub, Diamond Relat. Mater. **12**, 1477 (2003).
[24] J. Saida, M. Matsushita, and A. Inoue, Mater. Trans., JIM **42**, 1103 (2001).
[25] R. Z. Valiev and I. V. Alexandrov, Defect Diffus. Forum **208-2**, 141 (2002).